Plume and Finger Regimes Driven by an Exothermic Interfacial Reaction

Kerstin Eckert[1] and Alexander Grahn[2]
[1]*Institute for Aerospace Engineering, Dresden University of Technology, 01062 Dresden, Germany*
[2]*Institute for Safety Research, Research Center Rossendorf, P.O. Box 510 119, 01314 Dresden, Germany*

(Received 3 December 1998)

We study the pattern formation in a chemical two-layer system, placed in a Hele-Shaw cell. The upper layer is an organic solvent in which a carboxylic acid is dissolved. The lower layer consists of water containing an inorganic base. We report on a novel instability type which is driven by an exothermic neutralization reaction in vicinity to the interface. This instability combines plume and finger regimes and gives rise to a self-sustained dynamics. [S0031-9007(99)09292-3]

PACS numbers: 47.20.−k, 47.54.+r, 82.40.Ck

Studies of convection in fluids, such as Rayleigh-Bénard [1] or Bénard-Marangoni convection [2], have strongly influenced our understanding of pattern formation and turbulence. In these systems energy is supplied by an external temperature difference applied across a given length scale. However, this situation is not representative for a variety of systems occurring in nature. Here, the dynamics is driven by internal sources of energy and the selected length scale is a part of the solution of the problem. The study of such systems is interesting both from a fundamental point of view and with respect to potential applications of basic research. Promising candidates are systems involving chemical reactions. Consumption of educts and the release of reaction enthalpy provide sources of solutal and thermal gradients. Hydrodynamic instabilities, driven by these gradients, can drastically alter the chemical reaction rate.

There is an increasing interest in the interaction between traveling *chemical fronts,* produced by an autocatalytic reaction, and convective flows [3–5]. One focus of those works is on the onset of buoyancy driven convection. Hydrodynamic instabilities due to a reaction at a physical *interface* were the subject of several theoretical studies [6,7]. The latter provide a detailed analysis of the the coupling between chemical reaction and Marangoni convection, driven by concentration gradients along the interface. The acceleration of interfacial reactions by convection was first observed experimentally in [8]. The pattern formation at liquid-gas interfaces driven by photochemical reactions was studied in [9]. However, concerning the interplay between a *nonisothermal* reaction at a *liquid-liquid* interface and convection, we are not aware of any further experimental work. In the present paper we demonstrate that a rather simple interfacial neutralization reaction can develop an unexpected coupling of different hydrodynamic instabilities. Among these are boundary layer and double diffusive finger instabilities.

The experiments were performed in a two-layer system, placed in a Hele-Shaw cell (Fig. 1). The gap width was $d = 0.1$ cm. In the majority of the experiments the Hele-Shaw cells were operated in the vertical position. The two-layer system inside the cell consisted of a lower aqueous layer (water and base) and an upper organic layer (isobutyl alcohol and carboxylic acid). The viscosity of the organic solvent is 4 times higher than that of water. Since water and isobutyl alcohol have a certain solubility (12% at $T = 25\,^\circ\mathrm{C}$) saturated solutions were prepared before filling. Saturation was to prevent interfacial turbulence arising from counterdiffusion of the solvents into each other. While the concentration of the base B in the water was fixed to $c_B = 1$ mol/l, different concentrations, $c_{\mathrm{H}A}$, of the acids, HA, have been used ($c_{\mathrm{H}A} = 0.04$ to 0.08 g/l or equivalently 0.5 to 2 mol/l).

Filling was done by means of syringes. To achieve a careful pouring of the organic layer onto the aqueous one we used stainless-steel bows with a thickness of 0.08 cm and of a length $L \sim X$ (cf. Fig. 1). The bow was placed 1.5 cm above the lower layer. It was slowly pulled out when filling of the organics began. By injecting the fluid past the bow, a quasihomogeneous growth of the upper layer was achieved, while most of the momentum of the fluid was buffered by the bow. Visualization of the pattern was done by means of a shadowgraph technique.

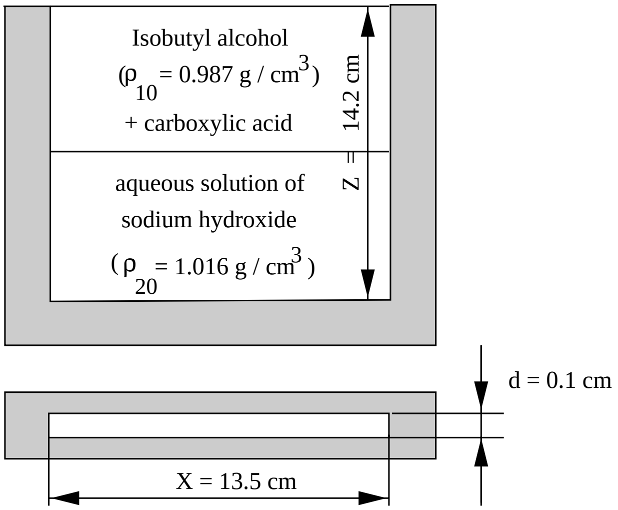

FIG. 1. The two-layer system in the Hele-Shaw cell. The given densities refer to the saturated phases.

The basic reaction is the neutralization of a carboxylic acid by a base, sodium hydroxide, close to the interface. A precondition of this reaction is the dissociation of both species, i.e.,

$$\mathrm{H}A + \mathrm{H_2O} \rightleftharpoons A^- + \mathrm{H_3O^+} \quad \text{with } K_a = \frac{c_{\mathrm{H}^+} c_{A^-}}{c_{\mathrm{H}A}}, \tag{1}$$

$$B + \mathrm{H_2O} \rightleftharpoons B\mathrm{H}^+ + \mathrm{OH}^- \quad \text{with } K_b = \frac{c_{B\mathrm{H}^+} c_{\mathrm{OH}^-}}{c_B}. \tag{2}$$

K_a and K_b are the dissociation constants. While sodium hydroxide as a strong base has a high K_b, the K_a values of the weak organic acids are small (Table I). This means that only a small amount, $\gamma \approx 1\%$, of the acid dissociates. The dissociation degree γ decreases with decreasing K_a. If a hydronium ion, formed by (1), encounters a OH^--ion neutralization takes place, i.e.,

$$\mathrm{H_3O^+} + \mathrm{OH^-} \rightleftharpoons 2\mathrm{H_2O}, \tag{3}$$

where the equilibrium prefers the product. The released reaction enthalpy amounts to $\Delta H \approx -57$ kJ/mol. Because of the low K_a values, the sodium and the acetate ions (in case of acetic acid) remain dissociated; i.e., no salt is formed. We use carboxylic acids with different chain lengths whose properties are given in Table I. The densities of the solutions, ρ_i $(i = 1, 2)$, are a function of the solute concentration (acid and base) and vary according to $\rho_i = \rho_{i0} + \beta_i c_{\mathrm{H}A}$, where $c_{\mathrm{H}A}$ is given in g/cm^3. Comparison with Table I shows that both densities increase with increasing acid concentration. Note that sodium hydroxide is insoluble in the organic solvent.

The system displays three basic regimes. The initial one (Fig. 2a) is dominated by rising *plumes* in the upper organic layer. The plumes are emitted from an unstable boundary layer above the interface. We assume that they consist of a warmer fluid with lower acid concentration. The intensity of the plume regime is most distinct in the formic-acid system and decreases with increasing chain length. The duration is of the order of minutes.

The intermediate regime (Fig. 2b) is characterized by plumes in the upper layer and by an irregular formation of fingers in the lower layer. The onset of the fingers starts earlier the longer the acid chain length is. The duration of this second regime is of the order of 1 hour. In its course the upper layer plume regime becomes increasingly disordered till it fades away.

TABLE I. Relevant material properties of the diffusing acids. ρ, $\bar{\beta}_1$, and $\bar{\beta}_2$ stand for density (at 20 °C [10]), average solutal volume expansion coefficient of isobutyl alcohol, and water, respectively ($\rho_i = \rho_{i0} + \bar{\beta}_i c_{\mathrm{H}A}$) [11]. K_a is the dissociation constant [12].

	Formic acid H-COOH	Acetic acid $\mathrm{CH_3}$-COOH	Propionic acid $\mathrm{C_2H_5}$-COOH
ρ (g/cm^3)	1.2204	1.0491	0.9934
$\bar{\beta}_1$	0.258	0.220	0.179
$\bar{\beta}_2$	0.233	0.103	0.083
K_a (mol/l)	1.77×10^{-4}	1.75×10^{-5}	1.34×10^{-5}

In the final regime (Fig. 2c) the system displays an array of regularly spaced *fingers*. In the fingers the warmer fluid, rich in acid/acetate ions, moves downwards [13]. In between the fingers the colder fluid, which should have a higher hydroxide concentration, moves in the opposite direction towards the interface. This is a double diffusive instability arising from the different diffusivities of heat and mass (cf. e.g., [14]). Since heat diffuses 100 times faster than the acid, the convective motion is driven by the horizontal concentration differences between the rising and falling fluid columns.

Next we analyze the upper-layer motions by studying the advancing of the plumes with time (Fig. 3). This is done by tracing the head positions of the plumes in the digitized shadowgraph images and averaging over the plume ensemble. Usually approximately ten plumes are taken into account. We find that the plume velocity decreases with increasing chain length. The error bars represent the standard deviation of the ensemble.

Let us now study the characteristic horizontal scale of the finger structure in the lower layer. To determine the wave number we apply one-dimensional Fourier transformation to lines parallel to the interface (512 pixels) and average over lines at different distances from interface. The corresponding power spectra are shown in Fig. 4. At equal molar concentrations, all three systems display nearly the same wave numbers k. After $\Delta t = 90$ min we find $k = (3.9 \pm 0.3)$ mm^{-1}. We could not detect a significant dependence on the gap width (0.5, 1.0, and 2.0 mm) of the Hele-Shaw cell. The corresponding vertical finger extension amounts to $h = (12 \pm 4)$ mm. h increases with advancing time which is accompanied by a decrease of the dominant finger wave number. Whether this decrease follows the $h^{-1/4}$ dependence, as known from thermohaline convection [14], is currently under study.

To develop ideas about the driving mechanisms several tests have been undertaken. First, we operate the Hele-Shaw cell in a horizontal instead of a vertical position to understand whether buoyancy or interfacial tension gradients are responsible for the pattern formation. We find that the pattern formation is nearly completely suppressed. Thus, the major part of the released potential energy emerges from buoyancy. We cannot completely exclude the influence of interfacial tension. Especially in the acetic-acid system rather intensive motions exist in close vicinity to the interface. They seem to provide an additional propulsion of the global motions driven by buoyancy.

In a second step we omit the base in the lower layer. The characteristic feature of this pure mass transfer case is an inverted plume regime in the lower layer (Fig. 5).

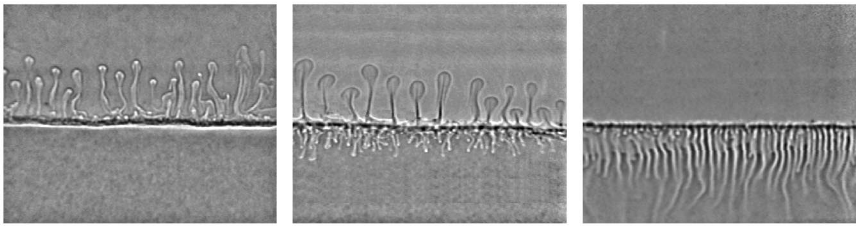

(a) (b) (c)

FIG. 2. The three regimes. (a) Rising plumes; (b) plumes and irregular fingers; (c) nearly regular fingers. The diffusing acids are formic acid (a) and propionic acid [(b)–(c)]. The regimes are present in all three acid systems.

The phenomenology in the upper layer, however, depends on the diffusing acid. The acetic- and the propionic-acid systems show a diffusing interface (cf. Fig. 5). It moves slowly away from the interface whereby its contours become increasingly modulated. In contrast to that, the formic-acid system displays a plume regime which resembles that of Fig. 2a. If we compare the advancing of this plume ensemble with and without reaction we find an acceleration of the plume ensemble in the first case. Thus, the rising of the plumes is both a solutal and a thermal effect. To support this idea we have placed the Hele-Shaw cells into a larger transparent box fed with a water flow of reduced temperature ($T = 14.5\ ^\circ\mathrm{C}$) to allow a faster removal of heat through the walls of the cell. Here, we find a slowing down of the plume rising by at least 20%. Although the temperature reduction also influences solubility and viscosity, this observation gives a hint that a large part of the released potential energy is provided by thermal buoyancy.

The engine of the dynamics described above is the diffusion of the acid from the upper into the lower layer. Since both β_1 and β_2 are greater than zero (Table I) unstable density stratifications are developed at both sides of the interface. Let us first discuss the simpler case of pure mass transfer without reaction (Fig. 5). In the lower layer, the heavier concentration boundary layer, henceforth abbreviated by b.l., is intrinsically unstable. Convection in the form of inverted plumes sets in. This is similar to the instability due to evaporative cooling of an initially isothermal layer [15] or due to viscous Rayleigh-Taylor instability at vanishing interfacial tension [16]. Convective motions in the lower layer cause a higher acid flux through the interface. Consequently, the acid concentration gradient across the upper b.l. increases. The control parameter determining the stability of this b.l. is the solutal Rayleigh number, Ra_s, defined as $\mathrm{Ra}_s = (\beta_1 g \delta^3 \Delta c_{\mathrm{HA}})/\nu D$, based on the upper b.l. thickness δ. (g, ν, and D stand for gravitional acceleration, viscosity, and mass diffusion coefficient.) If the critical value $\mathrm{Ra}_s \sim 10^3$ is exceeded the b.l. becomes unstable. This is in close analogy to the instability of a thermal b.l. on a heated plate [17].

Let us now consider the system with chemical reaction. As soon as acid enters the aqueous phase it instantaneously dissociates to a small part according to (1). If now a $\mathrm{H_3O^+}$ ion encounters a $\mathrm{OH^-}$ ion a neutralization reaction (3) takes place. This is known to be one of the fastest solution reactions since both ions do not undergo conventional diffusion [18]. Thus, the neutralization rate is controlled by the diffusion of acid *into* water.

The exothermicity of the reaction (3), given by ΔH, drastically modifies the phenomenolgy of the mass-transfer

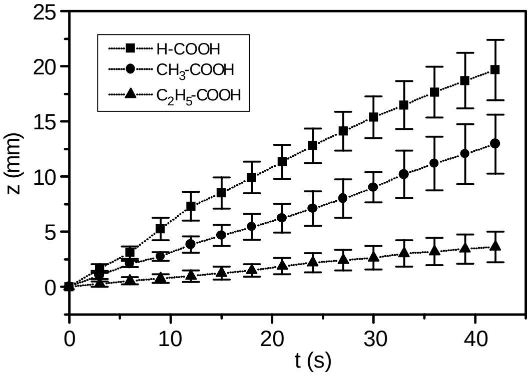

FIG. 3. Advancing of the plume ensemble with time for the three diffusing acids ($c_{HA} = 0.08$ g/l).

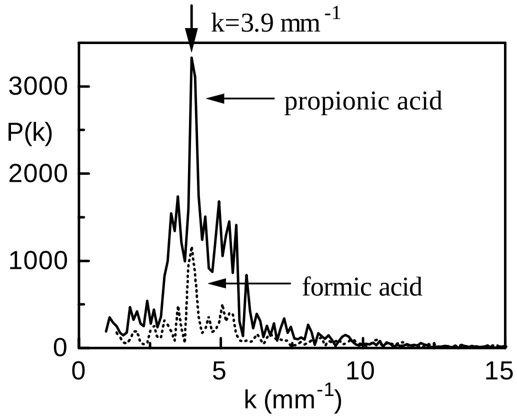

FIG. 4. One-dimensional power spectra of the fingers ($c_{\mathrm{HA}} = 1$ mol/l). Note that the basic modes have the same k. For the sake of clarity we omit the acetic-acid system whose curve lays between that of formic and propionic acids.

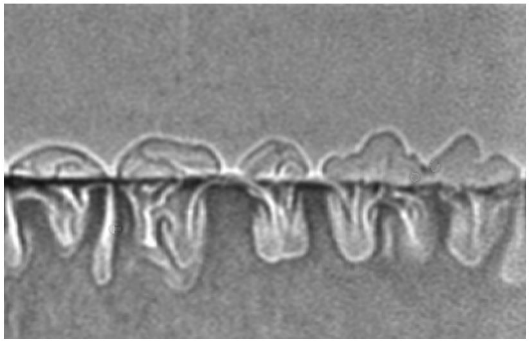

FIG. 5. Pattern formation during pure mass transfer of acetic acid (no reaction, $c_{HA} = 1$ mol/l).

case: The diffusive interface (acetic-acid/propionic-acid systems) in the *upper layer* becomes unstable to eject plumes. Solutal plumes in the formic-acid system move faster due to additional thermal buoyancy. The reason for the different velocities of the plume ensembles (Fig. 3) must be sought in the different K_a values of the acids. The higher the dissociation degree the higher the available thermal buoyancy.

However, the most surprising consequence of the chemical reaction is the crossover from the regime of inverted plumes to the finger regime in the *lower layer*. The condition for finger formation reads $(\beta_2 \partial c_{\mathrm{HA}}/\partial z)/|\alpha \rho_0 \partial T/\partial z| > D/\kappa$ (cf. e.g., [14]). κ and α denote thermal diffusivity and thermal expansion. Let us briefly show that it is simple for the system to fulfill this condition: The typical time for onset of instability is $t_c \sim 10$ s. For the acid gradient below the interface the approximate relation $\Delta c_{\mathrm{HA}}/\delta_c = 10^{-1}\ \mathrm{mol\,cm^{-4}}$ holds, where $\Delta c_{\mathrm{HA}} \sim 1\ \mathrm{mol\,l^{-1}}$ and the concentration b.l. thickness, δ_c, is $\delta_c \sim \sqrt{D t_c}$. According to Fick's diffusion law, we find for the acid flux into water $\Delta n_{\mathrm{HA}}/\Delta t = D A \Delta c_{\mathrm{HA}}/\delta_c \sim 10^{-6}\ \mathrm{mol\,s^{-1}}$ (interfacial area $A \sim 1\ \mathrm{cm}^2$, $D \sim 10^{-5}\ \mathrm{cm^2/s}$). Thus, the production rate of H_3O^+ ions in the concentration b.l. is $\Delta c_{\mathrm{H_3O^+}}/\Delta t = \gamma \Delta n_{\mathrm{HA}}/(\Delta t A \delta_c) \sim 10^{-6}\ \mathrm{mol\,cm^{-3}\,s^{-1}}$. By multiplying this with $\Delta H/(\rho c_p)$ (c_p—heat capacity) we obtain a temperature gradient $\Delta T/\delta_{\mathrm{th}} \sim -1$ K/cm after time t_c; the thermal b.l. thickness is $\delta_{\mathrm{th}} \sim \sqrt{\kappa t_c}$. (Note that heat conduction through the walls was neglected.) Inserting these values into the left-hand side of the finger condition we obtain 10^2 while $D/\kappa \sim 10^{-2}$. Thus, the conditions provided by this exothermic interface reaction are strongly conducive to finger formation.

We expect that numerous interfacial reactions are accompanied by the formation of fingers and plumes. Since both instabilities lead to an efficient mixing they can strongly accelerate diffusion-controlled interfacial reactions. Thus, the understanding of the hydrodynamics offers a possibility to control this reaction type. Furthermore, the discussed class of systems can serve as a model for studies of self-sustained dynamics.

We are grateful to I. Steinrücken, H. Bernsmann, B. Plietker, A. A. Golovin, A. De Wit, A. Thess, R. Schaller, H.-M. Prasser, and R. Grundmann for fruitful discussions. K. E. and A. G. acknowledge financial support by the Deutsche Forschungsgemeinschaft, Grants No. Th497/8-1 and No. Pr488/3-1, and by Deutsches Zentrum für Luft- und Raumfahrt (K. E.).

[1] M. C. Cross and P. C. Hohenberg, Rev. Mod. Phys. **65**, 851 (1993).

[2] E. L. Koschmieder, *Bénard Cells and Taylor Vortices* (Cambridge University Press, Cambridge, England, 1993); K. Eckert, M. Bestehorn, and A. Thess, J. Fluid Mech. **356**, 155 (1998), and references therein.

[3] J. A. Pojman and I. R. Epstein, J. Phys. Chem. **94**, 4966 (1990), and references therein.

[4] Y. Wu, D. A. Vasquez, B. F. Edwards, and J. W. Wilder, Phys. Rev. E **52**, 6175 (1995); D. A. Vasquez and C. Lengacher, Phys. Rev. E **58**, 6865 (1998).

[5] B. S. Martincigh, M. J. B. Hauser, and R. H. Simoyi, Phys. Rev. E **52**, 6146 (1996), and references therein.

[6] E. Ruckenstein and C. Berbente, Chem. Eng. Sci. **19**, 329 (1964); W. Dalle Vedove and A. Sanfeld, J. Colloid Interface Sci. **84**, 318 (1981), and references therein.

[7] Yu. A. Buyevich, L. M. Rabinovich, and V. Vyazmin, J. Colloid Interface Sci. **173**, 1 (1995); L. M. Pismen, Phys. Rev. Lett. **78**, 382 (1997), and references therein.

[8] T. S. Sherwood and J. C. Wei, Ind. Eng. Chem. **49**, 1034 (1957).

[9] D. Avnir and M. L. Kagan, Chaos **5**, 589 (1995).

[10] J. Timmermans, *Physico-Chemical Constants of Pure Organic Compounds* (Elsevier Publishing Company, New York, 1950).

[11] A. Grahn and K. Eckert (unpublished).

[12] R. Brdicka, *Grundlagen der Physikalischen Chemie* (Deutscher Verlag f. Wissenschaften, Berlin, 1962).

[13] The bright appearing fingers must contain fluid of a higher refraction index n ($n_{\mathrm{water}} = 1.33 < n_{\mathrm{acid}} = 1.38$).

[14] C. Y. Shen, Phys. Fluids A **1**, 829 (1989), and references therein.

[15] W. G. Spangenberg and W. R. Rowland, Phys. Fluids **4**, 743 (1961).

[16] L. A. Newhouse and C. Pozrikidis, J. Fluid Mech. **217**, 615 (1990).

[17] L. N. Howard, in *Proceedings of the 11th International Congress of Applied Mechanics, Munich, Germany, 1964* (Springer, Berlin, 1966), p. 1109.

[18] P. W. Atkins, *Physical Chemistry* (W. H. Freeman and Company, San Francisco, 1978).